THE JOURNAL OF COMPARATIVE NEUROLOGY 465:179–194 (2003)

Zonal Organization of the Vestibulocerebellum in Pigeons (*Columba livia*): III. Projections of the Translation Zones of the Ventral Uvula and Nodulus

DOUGLAS R.W. WYLIE,[1,2]* MATTHEW R. BROWN,[2] IAN R. WINSHIP,[1]
NATHAN A. CROWDER,[2] AND KATHERINE G. TODD[2,3]
[1]Department of Psychology, University of Alberta, Edmonton, Alberta T6G 2E9, Canada
[2]Division of Neuroscience, University of Alberta, Edmonton, Alberta T6G 2E9, Canada
[3]Neurochemical Research Unit, Department of Psychiatry, University of Alberta, Edmonton, Alberta T6G 2E9, Canada

ABSTRACT

Previous electrophysiological studies in pigeons have shown that the complex spike activity of Purkinje cells in the medial vestibulocerebellum (nodulus and ventral uvula) is modulated by patterns of optic flow that result from self-translation along a particular axis in three-dimensional space. There are four response types based on the axis of preferred translational optic flow. By using a three axis system, where +X, +Y, and +Z represent rightward, upward, and forward self-motion, respectively, the four cell types are t(+Y), t(–Y), t(–X–Z), and t(–X+Z), with the assumption of recording from the left side of the head. These response types are organized into parasagittal zones. In this study, we injected the anterograde tracer biotinylated dextran amine into physiologically identified zones. The t(–X–Z) zone projected dorsally within the vestibulocerebellar process (pcv) on the border with the medial cerebellar nucleus (CbM), and labeling was found in the CbM itself. The t(–X+Z) zone also projected to the pcv and CbM, but to areas ventral to the projection sites of the t(–X–Z) zone. The t(–Y) zone also projected to the pcv, but more ventrally on the border with the superior vestibular nucleus (VeS). Some labeling was also found in the dorsal VeS and the dorsolateral margin of the caudal descending vestibular nucleus, and a small amount of labeling was found laterally in the caudal margin of the medial vestibular nucleus. The data set was insufficient to draw conclusions about the projection of the t(+Y) zone. These results are contrasted with the projections of the flocculus, compared with the primary vestibular projection, and implications for collimotor function are discussed. J. Comp. Neurol. 465:179–194, 2003.

Indexing terms: vestibulocerebellum; optokinetic; Purkinje cells; vestibular nuclei; cerebellar nuclei; anterograde tracer

Previous neurophysiological research in pigeons has shown that the complex spike activity (CSA) of Purkinje cells in the vestibulocerebellum (VbC) responds to particular patterns of optic flow that result from self-motion. CSA in the lateral VbC (i.e., the flocculus) responds best to optic flow that results from self-rotation about either the vertical axis or a horizontal axis oriented at 45° contralateral azimuth (Wylie and Frost, 1993; see also Simpson et al., 1981; Graf et al., 1988; Leonard et al., 1988; Winship and Wylie, 2001). CSA in the medial VbC of pigeons (i.e., the ventral uvula and nodulus) responds best to optic flow that results from self-translation along a particular axis in three-dimensional space (Wylie et al., 1993; Wylie and Frost, 1999a). With respect to the preferred axes of translational optic flow, there are four response types. The orientation of the best axis for each of the four types is described using the reference frame depicted in Figure 1. *X*, *Y*, and *Z* represent the interaural, vertical, and naso-

Grant sponsor: Natural Sciences and Engineering Research Council of Canada (NSERC) (D.R.W.W., I.R.W., N.A.C.); Grant sponsor: the Canadian Institute for Health Research (CIHR); Grant sponsor: Davey Endowment for Brain Injury Research (K.G.T.); Grant sponsor: the Alberta Heritage Foundation for Medical Research (M.R.B.).

*Correspondence to: Douglas R. Wong-Wylie, Department of Psychology, University of Alberta, Edmonton, Alberta T6G 2E9, Canada.
E-mail: dwylie@ualberta.ca

Received 7 November 2002; Revised 4 February 2003; Accepted 12 February 2003

DOI 10.1002/cne.10857

Published online the week of August 25, 2003 in Wiley InterScience (www.interscience.wiley.com).

occipital axes, respectively. With respect to direction, $+X$, $+Y$, and $+Z$ represent rightward, upward, and forward self-translation, respectively. Neurons respond best to optic flow patterns resulting from either upward or downward self-translation along the vertical axis [t(+Y) and t(–Y) neurons] or self-translation along one of two horizontal axes oriented 45° to the midline [t(–X–Z) and t(–X+Z) neurons, assuming recording from the left VbC; Wylie et al., 1998; Wylie and Frost, 1999a].

Electrophysiological studies have shown that the four response types in the medial VbC are organized into parasagittal zones. t(–X–Z) responses are found in a zone that abuts the midline and is about 0.5 mm in width, and t(–X+Z) responses are found in the adjacent zone, 0.5–1.0 mm from the midline (Wylie and Frost, 1999a). t(–Y) units are found in a zone lateral to this (Wylie et al., 1993; Wylie and Frost, 1999a). t(+Y) responses are uncommon, although it has been suggested, with caution, that they are found lateral to the t(–Y) responses (Wylie and Frost, 1999a; Crowder et al., 2000). Crowder et al. (2000), using the retrograde tracer cholera toxin subunit B (CTB), found that the four different response types received climbing fiber (CF) input from discrete regions of the medial column of the inferior olive (IO). The topographic organization in the IO was confirmed with electrophysiological recordings (Winship and Wylie, 2001).

Wylie et al. (1999a) showed that the translation-sensitive Purkinje cells in the medial VbC project to several sites in the vestibular and cerebellar nuclei (see also Arends and Zeigler, 1991a). After injections of the anterograde tracer biotinylated dextran amine (BDA) into the medial VbC, heavy terminal labeling was seen in the superior vestibular nucleus (VeS), the descending vestibular nucleus (VeD), the medial cerebellar nucleus (CbM), and the cerebellovestibular process (pcv). A consistent, but weaker, projection to the medial vestibular nucleus (VeM) was also observed, and, in a few cases, sparse labeling was seen in the tangential vestibular nucleus (Ta), the dorsolateral vestibular nucleus (VDL), and the lateral vestibular nucleus pars ventralis (VeLv). In the present study, BDA was injected into physiologically identified zones of the medial VbC in attempt to determine whether the different response types have different projection patterns.

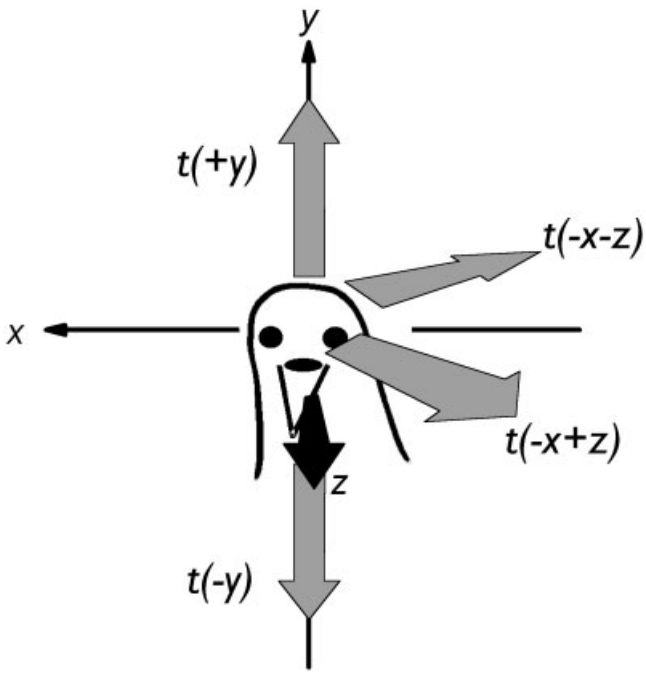

Fig. 1. Processing of translational optic flow in the medial vestibulocerebellum (VbC) of pigeons. The complex spike activity (CSA) of Purkinje cells in the medial VbC responds best to translational optic flow. The best response axes are illustrated with respect to a reference frame in which $+X$, $+Y$, and $+Z$ represent rightward, upward, and forward self-translational, respectively. The gray arrows represent the direction in which the animal would translate to produce the flow field that elicits maximal CSA. The four response types are t(+Y), t(–Y), t(–X–Z), and t(–X+Z). See text for details.

Abbreviations

An	nucleus angularis
CbL	lateral cerebellar nucleus
CbM	medial cerebellar nucleus
CF	climbing fiber
CSA	complex spike activity
CTB	cholera toxin subunit B
dIXcd	folium IXcd, dorsal lamella
dX	folium X, dorsal lamella
fI	folium I
gl	granule layer
Inf	infracerebellar nucleus
La	nucleus laminaris
MC	nucleus magnocellularis
ml	molecular layer
nBOR	nucleus of the basal optic root
nIX	nucleus of the glossopharyngeal nerve
nX	nucleus of the vagus nerve
PCV/pcv	cerebellovestibular process
PH/ph	nucleus prepositus hypoglossi
Pl	Purkinje layer
Ta	tangential nucleus
VbC	vestibulocerebellum
VDL	dorsolateral vestibular nucleus
VDN	ventral dentate nucleus
VeD	descending vestibular nucleus
VeLd	lateral vestibular nucleus, pars dorsalis
VeLv	lateral vestibular nucleus, pars ventralis
VeM	medial vestibular nucleus
VeS	superior vestibular nucleus
vIXcd	folium IXcd, ventral lamella
vX	folium X, ventral lamella
wm	cerebellar white matter

MATERIALS AND METHODS

The methods reported herein conformed to the guidelines established by the Canadian Council on Animal Care and were approved by the Biosciences Animal Care and Policy Committee at the University of Alberta. Silver king and homing pigeons (obtained from a local supplier) were anesthetized with a ketamine (65 mg/kg)-xylazine (8 mg/kg) cocktail (i.m.). Supplemental doses were administered as necessary. The animals were placed in a stereotaxic device with pigeon ear bars and beak adapter so that the orientation of the skull conformed to the atlas of Karten and Hodos (1967). Access to the VbC was achieved by removing bone and dura overlying the dorsal surface of the cerebellum and using the stereotaxic coordinates of Karten and Hodos (1967). Glass micropipettes, filled with 2M NaCl and having tip diameters of 4–5 μm were in-

serted to record the CSA of Purkinje cells. Electrodes were advanced using a hydraulic microdrive (Frederick Haer & Co.). Extracellular signals were amplified, filtered, and fed to a window discriminator that produced TTL pulses, each representing a single spike time. TTL pulses were fed to a data analysis system [Cambridge Electronic Designs (CED) 1401plus], and peristimulus time histograms (PSTHs) were constructed by using Spike2 software (CED).

CSA can be easily identified based on the low firing rate of about 1 spike/second. After a cell was isolated, the optic flow preference of the CSA was determined by moving a large (90° × 90°) hand-held stimulus in various areas of the visual field and by monitoring responses to translational flow-field stimuli produced by a planetarium projector, described elsewhere (Wylie et al., 1998; Wylie and Frost, 1999b). Generally, we found that the most convenient way to identify the flow field preference was to use a computer-generated large-field stimulus and a procedure that is illustrated in Figure 2 (Winship and Wylie, 2001; Winship and Wylie, 2003; Wylie et al., 2003). A screen measuring 90° × 75° (width × height) was positioned in one of three locations relative to the bird's head: the frontal visual field [from 45° ipsilateral (i) to 45° contralateral (c) azimuth], the contralateral hemifield (from 45°c to 135°c azimuth), or the ipsilateral hemifield (from 45°i to 135°i azimuth; see Fig. 2A). Drifting square wave or sine wave gratings of an effective spatial and temporal frequency were then generated by a VSGThree (Cambridge Research Services) and back-projected (InFocus LP750) onto the screen. Direction tuning curves in each of the three areas of the visual field were obtained by moving the gratings in eight different directions. Responses were averaged over at least three sweeps, in which each sweep consisted of 5 seconds of motion in one direction, a 5-second pause, and 5 seconds of motion in the opposite direction, followed by a 5-second pause. Although this procedure did not elicit maximal modulation of the cell, it was quite useful for identifying the four different response types (see below; Fig. 2B,C).

After we identified the flow field preference of the CSA, the recording electrode was replaced with a pipette (tip diameter 10–20 μm) containing BDA [Molecular Probes, Eugene, OR; molecular weight 10,000; 10% in 0.1M phosphate buffer (PB; pH 7.4)] that was iontophoretically injected (+3 μA, 1 second on, 1 second off) for between 2 and 5 minutes. A short injection time was used to keep the size of the injection as small as possible, thereby increasing our confidence that the injection was confined to a single zone. After the injection, the electrode was left undisturbed for an additional 5 minutes. The pipette was then removed, the wound was sutured, and the animal was allowed to recover.

After a survival time of 3 days, the animals were given an overdose of sodium pentobarbitol (100 mg/kg) and immediately perfused with saline (0.9%), followed by ice-cold paraformaldehyde (4% in 0.1M PB). The brains were extracted and postfixed for 2–12 hours (4% paraformaldehyde, 20% sucrose in 0.1M PB) and cryoprotected in sucrose overnight (20% in 0.1M PB). Frozen sections 44 μm thick were collected in the coronal plane. The BDA was visualized using a cobalt chloride intensification of diaminobenzidene. These procedures have been described in detail elsewhere (Wylie et al., 1997; see also Veenman et al., 1992; Wild, 1993). The tissue was mounted on gelatin

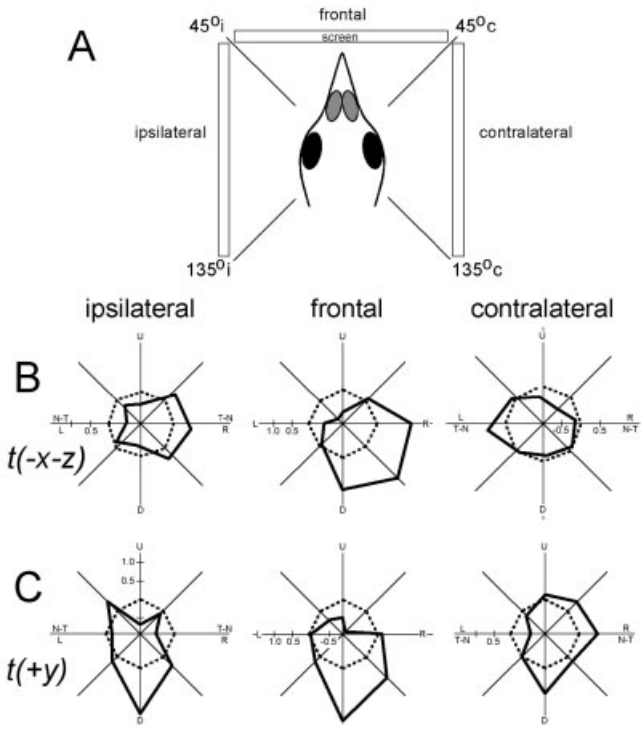

Fig. 2. Directional tuning of complex spike activity (CSA) of Purkinje cells to moving large-field sine-wave gratings presented in different regions of the visual field. Drifting gratings were back-projected onto a screen that measured 90° × 75° (width × height). As illustrated in **A**, the screen was positioned at one of three locations relative to the bird: the contralateral, ipsilateral, and frontal regions. Recordings were made from the left side of the brain. **B** and **C** show responses of t(–X–Z) and t(+Y) neurons, respectively, to the drifting gratings in each of the three regions. Polar plots of direction tuning are shown—firing rate [spikes/second re. spontaneous rate (SR)] as a function of the direction of large-field motion. The dashed circles represent the SR (set to 0 spikes/second). U, D, L, and R are upward, downward, leftward, and rightward motion, respectively; N-T and T-N, nasal-to-temporal and temporal-to-nasal motion, respectively; i, ipsilateral; c, contralateral.

chrome aluminium-coated slides, lightly counterstained with neutral red, and examined by using light microscopy.

The photomicrographs shown in Figure 4 were taken using a compound light microscope (Olympus Research Microscope BX60) equipped with a digital camera (Media Cybernetics CoolSNAP-Pro color digital camera). Adobe Photoshop was used to compensate for brightness and contrast. Tracings in Figures 5–9 were constructed using a drawing tube, scanned into digital format (Epson Perfection 1200), and formatted in Adobe Photoshop. Sections throughout the extent of the cerebellar and vestibular nuclei were traced, although the number of tracings and distance between sections vary between figures. In these figures, each dot reflects the location of approximately five terminal varicosities.

Nomenclature

The avian cerebellum consists of a vermis without hemispheres, which is characteristic of mammalian species (Larsell, 1948; Larsell and Whitlock, 1952; Whitlock, 1952). The pigeon VbC consists of the two most ventral

folia of the posterior vermis: IXcd and X in the nomenclature of Karten and Hodos (1967), which we use, or IXb and X according to Arends and Zeigler (1991a, b). Generally, folia IXcd and X are referred to as the *uvula* and *nodulus*, respectively (Larsell, 1948; Larsell and Whitlock, 1952; Whitlock, 1952). These folia extend laterally and rostrally to form the auricle of the cerebellum, which has been referred to as the *paraflocculus* and/or *flocculus* (Larsell, 1948; Larsell and Whitlock, 1952; Whitlock, 1952). We define the flocculus as the lateral part of folia IXcd and X, where the CSA responds to rotational optic flow (Wylie and Frost, 1993; Wylie et al., 1993, 2003). More medially, CSA responds best to translational optic flow (Wylie et al., 1993, 1998; Wylie and Frost, 1999a). We refer to this area as the *ventral uvula* and *nodulus* or, collectively, as the *medial VbC*.

For the vestibular and cerebellar nuclei, we generally use the nomenclature of Karten and Hodos (1967), with a few exceptions. According to Karten and Hodos (1967), there are two cerebellar nuclei, the medial and lateral cerebellar nuclei (CbM, CbL), although CbM can be further subdivided. Arends and Zeigler (1991a, b) have identified a third nucleus, the infracerebellar nucleus (Inf), which is difficult to distinguish. Inf lies ventral and lateral to the rostral part of CbL and dorsal to the dorsolateral vestibular nucleus (VDL; see also Labendeira-Garcia et al., 1989; Arends et al., 1991a,b). The indistinct regions among the CbM, CbL, and vestibular complex are collectively referred to as the *cerebellovestibular process* (pcv). According to Karten and Hodos (1967), the vestibular nuclear complex consists of the VeM, the VeS, the VeD, the VeLd and VeLv, and the VDL. Dickman and Fang (1996) considered the VDL to be the dorsal extension of the VeLv. Dickman and Fang (1996) also identified groups A and B in pigeons, based on earlier studies in chickens (Wold, 1976). In our material, we could not reliably identify groups A and B, so they were not included in our analysis. The tangential nucleus (Ta) is a collection of large neurons that lies medially to the root of the vestibular nerve.

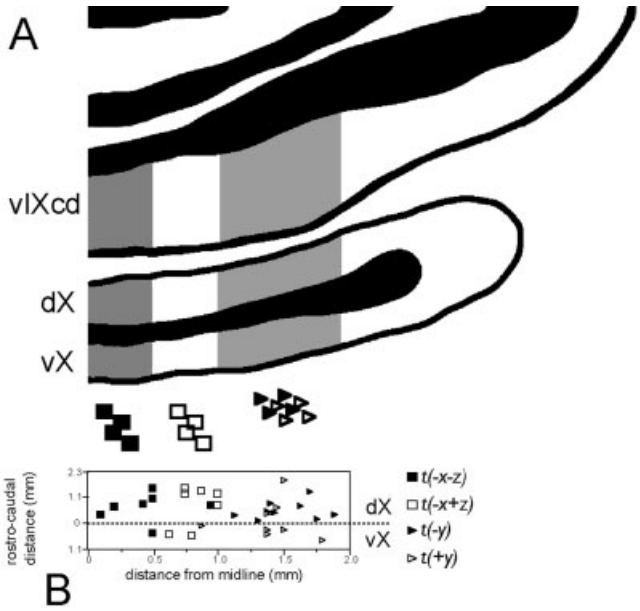

Fig. 3. Zonal organization of the medial vestibulocerebellum (VbC) in pigeons. **A** is a drawing of a coronal section through folia IXcd and X to show the zonal organization of the medial VbC. The most medial zone (dark gray) and the adjacent zone (white) are each about 0.5 mm in width and contain t(–X–Z) and t(–X+Z) cells, respectively. The third zone (light gray) is about 1 mm in width and contains both t(+Y) and t(–Y) cells. In **B**, the location of injection sites in the dorsal and ventral lamellae of folium X (dX, vX) from the present study and previous studies (Lau et al., 1998; Wylie et al., 1999a; Crowder et al., 2000) are shown. Both the rostrocaudal distance from the pole of folium X (0 mm) and the distance from the midline are indicated. See text for details.

RESULTS

Recordings and modulation of CSA in the medial VbC

CSA was reliably recorded and quantitatively identified as the t(–X–Z), t(–X+Z), t(–Y), or t(+Y) response type. Figure 2B and Figure 2C, respectively, show the direction tuning of CSA for individual t(–X–Z) and t(+Y) neurons in response to gratings drifting in the frontal, ipsilateral, and contralateral regions of the visual field. In the tuning curves, the firing rate (spikes/sec relative to the spontaneous rate) is plotted as a function of the direction of motion in polar coordinates (solid line). t(–X–Z) neurons were excited in response to large-field stimuli moving forward (temporal-to-nasal; T-N) in the contra- and ipsilateral visual fields and rightward motion in the frontal visual field[1] (assuming recording from the left VbC). As with the t(–X–Z) cells, t(–X+Z) cells preferred rightward motion in the frontal field but backward (nasal to temporal; N-T) motion in the ipsilateral and contralateral fields (not shown). t(+Y) neurons were excited in response to large-field stimuli moving downward in all three visual fields (Fig. 2C). t(–Y) neurons were excited in response to large-field stimuli moving upward in all three visual fields (not shown).

Zonal organization of the medial VbC

In Figure 3, the zonal organization of the medial VbC is shown by using data obtained from the present study and previous neuroanatomical studies (Lau et al., 1998; Wylie et al., 1999a; Crowder et al., 2000). In these studies, deposits of BDA or CTB were injected at locations where the optic flow field preference of the CSA was determined. In Figure 3B, the locations of these injection sites in the dorsal and ventral lamellae of folium X (dX, vX) are shown. Both the rostrocaudal distance from the pole of folium X (0 mm) and the distance from the midline are indicated. [Data from the ventral lamella of folia IXcd (vIXcd; not shown) show the same pattern, although we have only half the number of data points]. From these data, a clear zonal organization is apparent. The most medial zone (dark gray in Fig. 3A) and the adjacent zone (white in Fig. 3A) are each about 0.5 mm in width and contain t(–X–Z) and t(–X+Z) cells, respectively. The third zone (light gray in Fig. 3A) is about 0.8–1.0 mm in width and contains both t(+Y) and t(–Y) cells. Both t(+Y) and t(–Y) were found in vIXcd (not shown) and dX, but t(–Y) cells were not found in vX (see Fig. 3B). For the present

[1]Note: The t(-X-Z) cell shown in 2B actually preferred rightward/downward motion in the frontal field.

study, we consider the projections of t(–Y) and t(+Y) cells separately.

Projections of the medial VbC

Experiments were performed on 19 animals. Sixteen birds received a unilateral injection and three received bilateral injections, but data from one of the bilateral cases (both injections) and five of the unilateral cases were discarded. Among these seven discarded injections, in five cases there was substantial spread of the injections to other folia (IXab, VIII and VII), and in the other two cases the CSA modulation was inconclusive. Thus the data set we describe includes 15 injections in 13 birds.

Figure 4A,B shows photomicrographs of two representative injection sites (from MB19 and MB2-left, respectively). It appeared that all 15 of the injection sites were confined to the molecular layer (ml) and Purkinje layer, but it is difficult to discount the possibility that some of the larger injections may have encroached upon the adjacent granular layer (see Discussion). The cells bodies (stylized arrows, Fig. 4A,B) and dendritic trees (smaller arrows, Fig. 4A,B) of a cluster of as few as 10 to as many as 90 Purkinje cells were labelled with each injection (see Table 1). At the center of the injection site, a beam of parallel fibers that traversed the folium and intersected the dendritic tree was also labelled (triangles in Fig. 4A). Retrogradely labelled granule cells were also observed (smallest arrows in Fig. 4B). In Table 1, several details of each injection site are shown: the optic flow preference of the CSA, the distance of the center of the injection from the midline, the number of labelled Purkinje cells, and the maximum width of the injection. There was extensive anterograde terminal labeling (i.e., varicosities) in the ipsilateral cerebellar and vestibular nuclei. Photomicrographs of labelled varicosities are shown in Figure 4C–L. The sites that received the heaviest terminal labeling were pcv (Fig. 4E,F; from MB7-left and MB1, respectively), CbM (Fig. 4G–I; from MB9-left), VeS (Fig. 4C,D; from MB7-left), and VeD (Fig. 4J–L; from MB7-left, MB7-left, and MB2-left, respectively). Terminal labeling was also occasionally seen in CbL, VeM, and VDL. There were three, five, five, and two injections in the t(–X–Z), t(–X+Z), t(–Y), and t(+Y) zones, respectively, and there were clear differences in the projection patterns of the different response types.

Figure 5 shows drawings of coronal sections (caudal to rostral) through the vestibular and cerebellar nuclei from case MB2. The distance (in μm) of each section relative to the rostralmost section is shown. In this and subsequent figures, the dots and stippling indicate the location of varicosities observed in five consecutive coronal sections, collapsed onto the central section. (Because the borders of the nuclei vary from section to section, special care was taken to ensure that the terminal labeling was assigned to the correct nuclei). There were two injection sites for this case, shown by the gray shading, both located in vIXcd (Fig. 5A). t(–Y) and t(–X+Z) cells were recorded on the left and right sides, respectively. On the left side, terminal labeling was heaviest ventrally in the pcv, especially on the border with the VeS (Fig. 5E–G), and within the caudal-dorsal tip of the VeS (Fig. 5F–H). A moderate amount of labeling was seen dorsolaterally in the caudal VeD (Fig. 5B–D), and this extended into the lateral margin of the caudal VeM (Fig. 5B). Sparse labeling was seen in the CbL (Fig. 5C,D) and the CbM (caudally, Fig. 5D–F). On the right side, the heaviest labeling was seen in the pcv, but more dorsally, on the border with the CbM (Fig. 5E–G). Moderate labeling was seen in the caudal CbM, particularly in the ventral half (Fig. 5D–F).

The patterns of terminal labeling from three of the other t(–X+Z) cases are shown in Figure 6. In case MB9 (Fig. 6F–J), the injection was quite small. Labeling was confined to the ventral margin of the caudal CbM (Fig. 6H) and dorsally in the pcv (Fig. 6I). The injection for case BDA26 (Fig. 6K–O) was larger, but generally the same pattern of labeling was seen in the CbM and pcv. In addition, a few varicosities were seen in the dorsal VeS (Fig. 6N,O) and VeD (Fig. 6K–M). The injection in case BDA27 (Fig. 6A–E) was quite large, and extremely heavy anterograde labeling was seen in the caudal CbM (Fig. 6C,D) and the adjacent dorsal pcv (Fig. 6C,D). Sparse labeling was also seen in the VeD (Fig. 6A,B), CbL (Fig. 6B,C), and dorsal VeS (Fig. 6D,E). Case MB7 (not shown) also had a large injection site, and the pattern of labeling was quite similar to that for case BDA27. In summary, from the five t(–X+Z) injections, labeling was consistently observed ventrally in the caudal CbM and dorsally in the pcv. We suggest that the sparse labeling in the dorsal VeS and VeD from the larger injections was a result of spread of the injections to the adjacent t(–Y) zone (see below).

Figure 7 shows the labeling from three other t(–Y) cases. The injection sites for cases MB11 and MB18 were both very small. For case MB11, the pattern of labeling was similar to that seen in case MB2-left. Labeling was most abundant ventrally in the pcv abutting the border of the VeS (Fig. 7H,I) and dorsally within the VeS (Fig. 7J). Some labeling was also observed in the dorsolateral VeD (Fig. 7H). For case MB18, very little anterograde labeling was found, but, consistent with the other cases, it was located ventrally in the pcv (Fig. 7N) and in the dorsal VeS (Fig. 7O). None was seen in the VeD. In case MB6, the injection was very large. Consistently with the other t(–Y) cases, labeling was found in the dorsal VeS and the adjacent pcv (Fig. 7D,E) and the dorsolateral VeD (Fig. 7B–D), and some was seen in the laterally in the caudal VeM (Fig. 7C). However, labeling was also seen dorsally in the pcv (Fig. 7C,D) and ventrally in the caudal CbM (Fig. 7C), as in the t(–X+Z) cases. In case MB7-left (not shown), the injection site was extremely large, and the anterograde labeling was extremely heavy. Heavy labeling was observed in the dorsal VeS and at two distinct sites in the pcv, one ventrally, consistently with the other t(–Y) cases, and one dorsally, as seen in the t(–X+Z) cases. A band of heavy labeling was also seen in the dorsal VeD, which extended into the caudolateral VeM. Sparse labeling was seen in CbL, Inf, and VDL and Ta. In summary, from the five t(–Y) injections, anterograde labeling was consistently observed ventrally in the pcv and in the adjacent dorsal VeS. A band of labeling was also seen in the dorsal VeD in all but one of the cases, and this extended into the caudolateral VeM in three cases.

Figure 8 shows the anterograde labeling from the three t(–X–Z) cases. In all cases, labeling was seen dorsally in the pcv (Fig. 8D,I,N), and, in cases MB19 and MB21, some labeling was also seen in the caudal CbM (Fig. 8H,I,M). In case MB19, there was a very small amount of labeling in VeD (Fig. 8G,H), but this could have resulted from the few Purkinje cells outside the VbC in dIXcd that were labelled in this case (Arends and Zeigler, 1991a). The labeling in

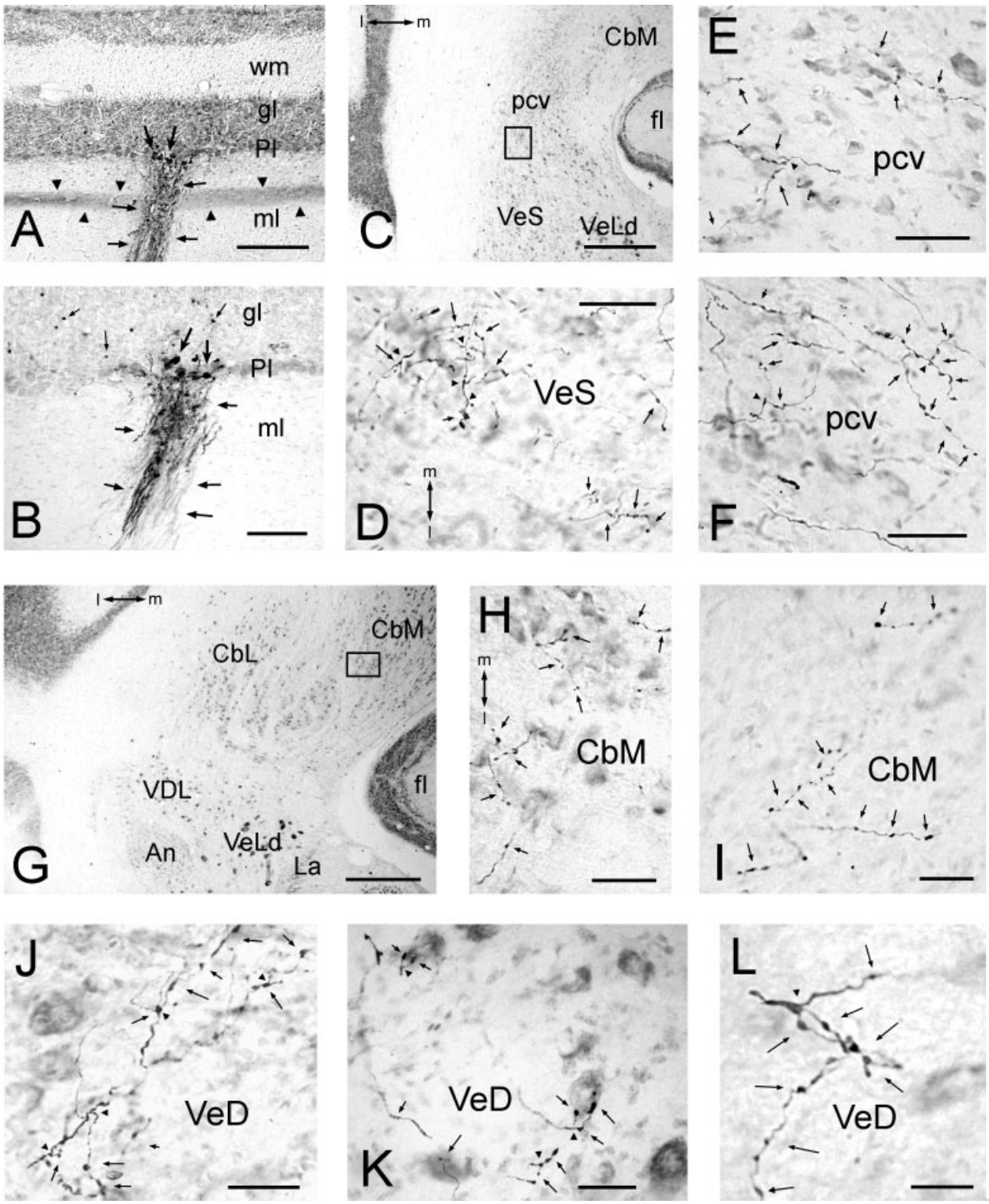

Fig. 4. In **A** and **B**, photomicrographs of two injection sites are shown. The injection site shown in A was located in the ventral lamella of folium IXcd (vIXcd) in the t(–X–Z) zone. The injection site shown in B was also located in the vIXcd, but more laterally, where t(–Y) CSA was recorded. In A and B, the stylized arrows indicate the somae of labelled Purkinje cells, and smaller arrows indicate the dendrites. In A, the triangles highlight the parallel fiber beam that transects the Purkinje cell dendrites. In B, the smallest arrows identify retrogradely labelled granule cells. **C–L** show examples of anterograde labeling in the vestibular and cerebellar nuclei. D shows labelled varicosities in the dorsal region of the caudal superior vestibular nucleus (VeS) on the border of the cerebellovestibular process (pcv). The area shown in D is indicated by the rectangle in C. Labelled varicosities in the pcv are shown in E and F. H and I show labelled varicosities in the ventral margin of the medial cerebellar nucleus (CbM). The area shown in H is indicated by the rectangle in G. Labelled varicosities in the descending vestibular nucleus (VeD) are shown in J–L. The arrows in C–L highlight labelled varicosities, and the triangles show clear branch points. m, medial; l, lateral. See list for other abbreviations. Scale bars = 200 μm in A; 100 μm in B; 500 μm in C,G; 50 μm in D,E,H; 30 μm in F,I–K; 15 μm in L.

TABLE 1. Details of the Injection Sites in the Medial Vestibulocerebellum (VbC)[1]

Case	CSA response	Distance (μm) of injection centre from midline	Injection width (μm)	No. of labelled VbC Purkinje cells
MB1	t(−X−Z)	575	160	30–35
MB19	t(−X−Z)	490	140	30–40[2]
MB21	t(−X−Z)	400	120	12–15
MB2-right side	t(−X+Z)	1,060	160	25–30
MB7-right side	t(−X+Z)	875	340	50–60[2]
MB9	t(−X+Z)	850	160	15–20
BDA26	t(−X+Z)	790	420	55–65[2]
BDA27	t(−X+Z)	760	560	75–90
MB2-left side	t(−Y)	1,330	100	30–35
MB6	t(−Y)	900	220	60–70
MB7-left side	t(−Y)	1,830	260	50–55[2]
MB11	t(−Y)	1,725	120	25–30
MB18	t(−Y)	1,625	200	30–40
MB22	t(+Y)	775	120	10–15
BDA28	t(+Y)	1,200	460	60–65

[1]For each injection site, the optic flow field preference of the complex spike activity (CSA), the location of the center of the relative to the midline, the maximal width of the injection, and the number of labelled Purkinje cells in the VbC are indicated.
[2]A few labelled Purkinje cells were also found outside VbC (<10).

the pcv and CbM in these cases was dorsal to that observed in the t(–X+Z) cases.

There were only two injection sites where t(+Y) CSA was recorded. [Previous studies have found that t(–Y) CSA is 10 times more common than t(+Y) CSA (Wylie and Frost, 1991; Wylie et al., 1993)]. The two t(+Y) cases are shown in Figure 9. In case MB22 (Fig. 9A–F), the injection was located 775 μm from the midline, which is characteristically the t(–X+Z) zone. In case BDA28 (Fig. 9G–L), the injection was centered 1,200 μm from the midline but was rather wide (460 μm). For both cases, the pattern of labeling bore some resemblance to both the t(–Y) and the t(–X+Z) cases. Labeling was seen ventrally in the caudal CbM (Fig. 9C,D,J) and both dorsally and ventrally within the pcv, extending into the dorsal VeS (Fig. 9C–F,J–L). Sparse labeling was seen in the lateral VeD (Fig. 9B,C,I,J), and a smattering of labeling was seen in the CbL (Fig. 9C,D,I,J).

DISCUSSION

Optic flow input to the vestibulocerebellum in birds and mammals

Optic flow analysis in brainstem visual systems begins with the retinal recipient nuclei in the pretectum and accessory optic system (AOS; for reviews see Simpson, 1984; Simpson et al., 1988a–c; Grasse and Cynader, 1990). In mammals, the AOS consists of the medial, lateral, and dorsal terminal nuclei, which collectively are equivalent to the nucleus of the basal optic root (nBOR) in birds (for reviews see Simpson, 1984; Weber, 1985; McKenna and Wallman, 1985). In the pretectum of mammals, the optic flow-sensitive cells are found in the nucleus of the optic tract (NOT), which is equivalent to the nucleus lentiformis mesencephali (LM) in birds. Although the projections of the pretectum and AOS are extensive (see, e.g., Brecha et al., 1980; Holstege and Collewijn, 1982; Giolli et al., 1984, 1985; Gamilin and Cohen, 1988; Simpson et al., 1988a, b; Blanks et al., 1995), it is the projection to the olivovestibulocerebellar pathway that has received the most attention. In mammals, the pretectum and AOS project to the dorsal cap and ventrolateral outgrowth of the inferior olive, which, in turn project as climbing fibers to the VbC (Mizuno et al., 1973; Takeda and Maekawa, 1976; Maekawa and Takeda, 1977, 1979; Holstege and Collewijn, 1982; Simpson, 1984; Giolli et al., 1985; Ruigrok et al., 1992; Blanks et al., 1995; Tan et al., 1995). In birds, the medial column of the inferior olive receives input from the LM and nBOR (Clarke, 1977; Brecha et al., 1980; Gamlin and Cohen, 1988; Wylie et al., 1997; Wylie, 2001) and projects to the VbC (Arends and Voogd, 1989; Lau et al., 1998; Wylie et al., 1999b; Crowder et al., 2000). Wylie (2001) emphasized that these pathways are highly conserved in birds and mammals. Most pretectal and AOS cells show direction selectivity to large-field stimuli but with receptive fields restricted to the contralateral eye (e.g., NOT: Collewijn, 1975; mammalian AOS: Simpson et al., 1979; LM: Winterson and Brauth, 1985; nBOR: Burns and Wallman, 1981; for reviews see Simpson, 1984; Simpson et al., 1988a; Grasse and Cynader, 1990). The olivary cells that receive input from the AOS and pretectum, and the CSA of Purkinje cells in the VbC have binocular, virtually panoramic receptive fields that respond to particular patterns of optic flow. This was first reported by Simpson et al. (1981), who showed that floccular CSA was modulated by rotational optic flow about either the vertical axis or a horizontal axis oriented at 45° contralateral azimuth (see also Leonard et al., 1988; Graf et al., 1988). Subsequently, Wylie and Frost (1993) reported virtually identical cell types in the flocculus of pigeons (see also Winship and Wylie, 2001). We refer to the two response types as *rVA* and *rH45* neurons, respectively. Simpson, Graf, and colleagues emphasized that optic flow cells of the flocculus, the vestibular canals, and the eye muscles all share a common frame of reference (Ezure and Graf, 1984; Graf et al., 1988; Leonard et al., 1988; Simpson and Graf, 1981, 1985; Graf and Simpson, 1981; Simpson et al., 1988a, b, 1989a, b; van der Steen et al., 1994; see also Wylie and Frost, 1996). In recent reports, we have shown that the zonal organization of the climbing fiber input to the rVA and rH45c zones in pigeons is similar to that in rabbits (Winship and Wylie, 2003), as are the projections of the rVA and rH45c zones to the vestibular and cerebellar nuclei (Wylie et al., 2003).

In contrast to the anatomy and physiology of the flocculus, the nodulus and ventral uvula are quite different in birds and mammals. The CF input to the uvula/nodulus in mammals is from the dorsal cap, ventrolateral outgrowth, and beta subnucleus, although there seem to be some discrepancies with respect to the zonal organization of these inputs in rabbits and rats (for review see Voogd et al., 1997). In mammals, there are visually responsive

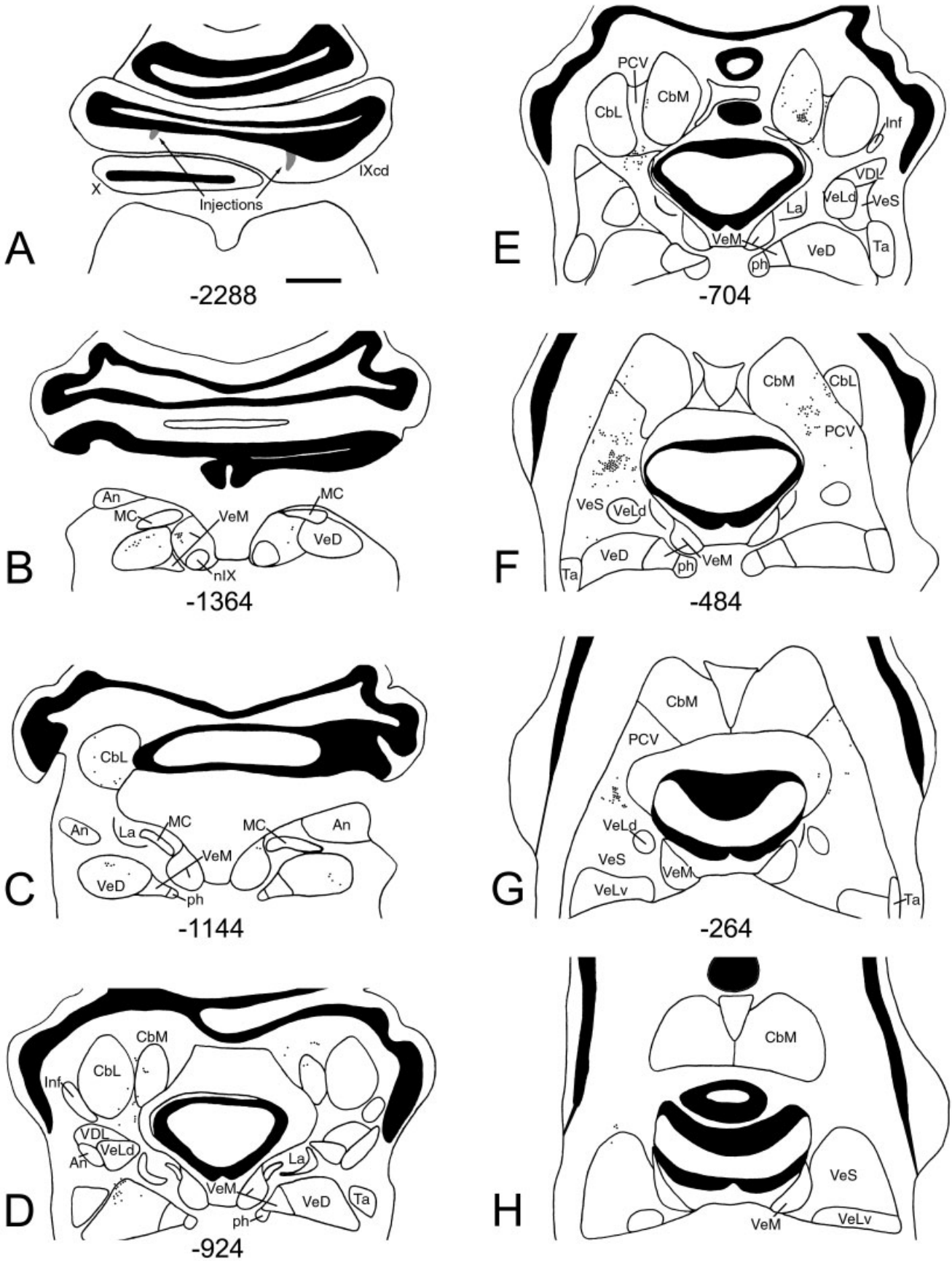

Fig. 5. **A–H:** Anterograde labeling from case MB2. Drawings of coronal sections (caudal to rostral) from case MB2 are shown. The distance of each section (in μm) from the rostralmost section is shown at the bottom of each panel. Both injections (gray shading) were located in the ventral lamella of folium IXcd. t(–Y) CSA was recorded at the injection site on the left side, and the injection on the right side was in the t(–X+Z) zone. The dots and stippling indicate the location of varicosities observed in five consecutive sections, collapsed onto the central section. See text for a detailed description. See list for abbreviations. Scale bar = 1 mm.

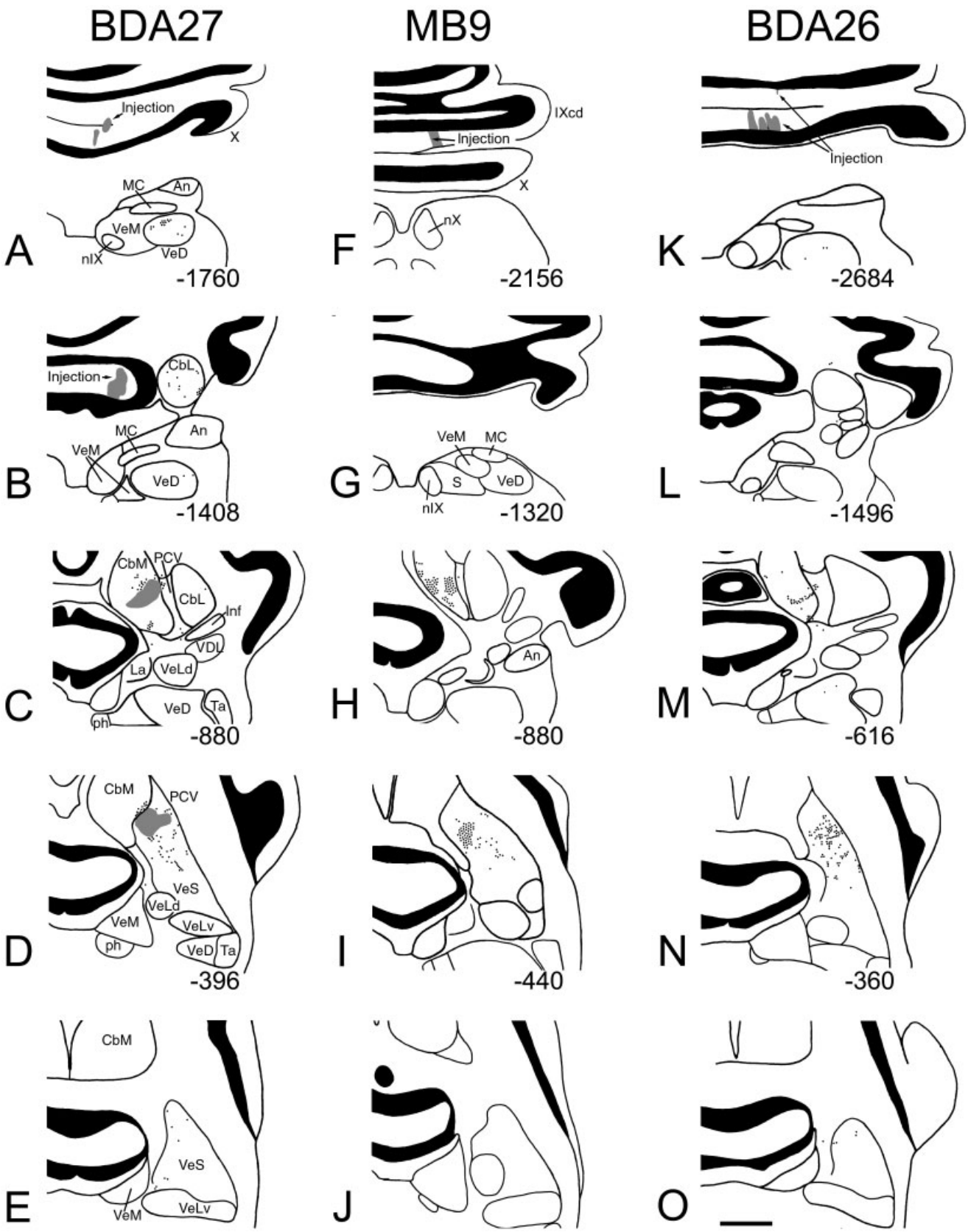

Fig. 6. **A–O:** Projections of Purkinje cells in the t(–X+Z) zone. Drawings of coronal sections (caudal to rostral) from cases BDA27 (left), MB9 (middle), and BDA26 (right) are shown. For additional details, see legend to Figure 5. See text for a detailed description. See list for abbreviations. Scale bar = 1 mm.

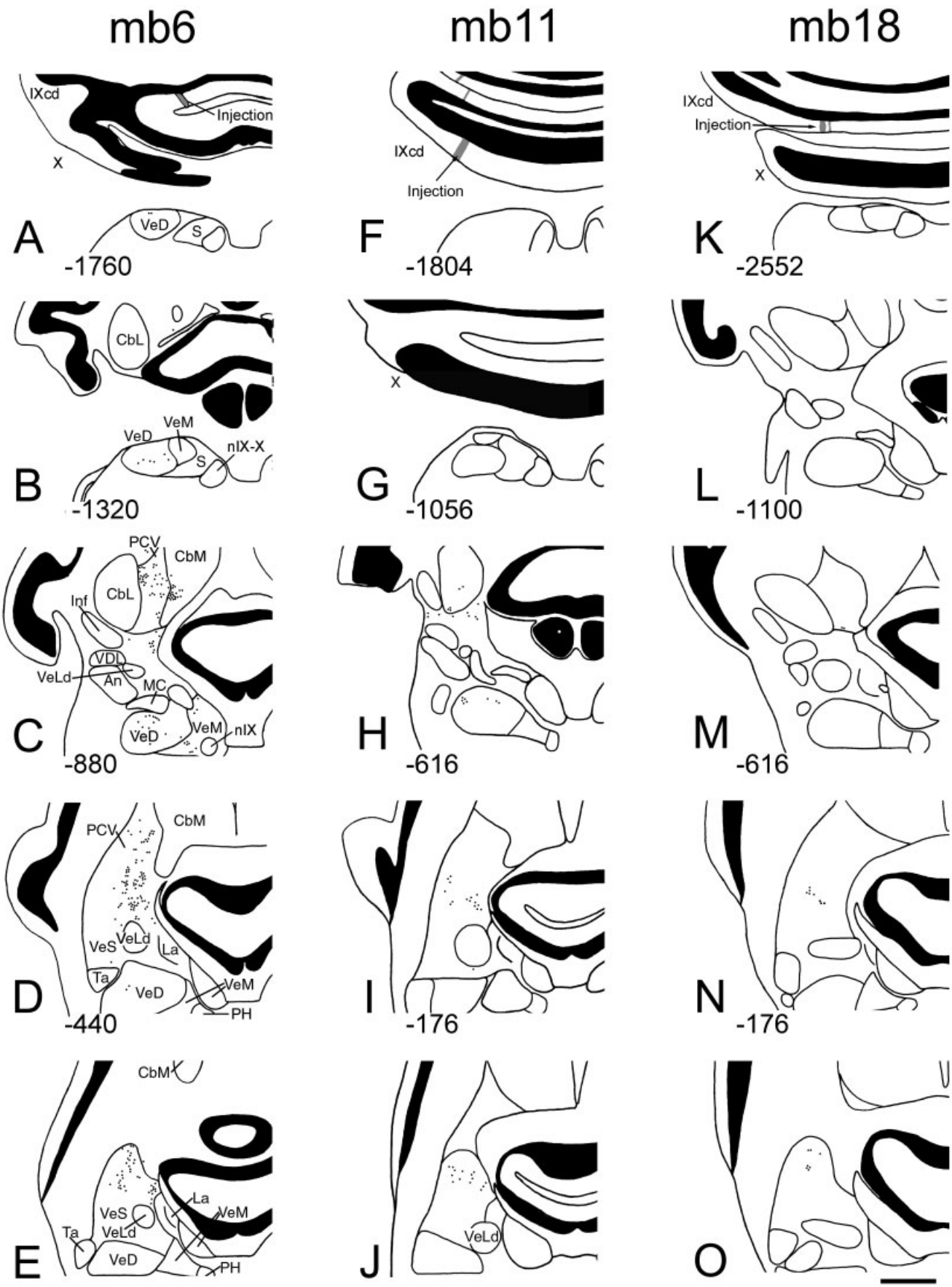

Fig. 7. **A–O:** Projections of Purkinje cells in the t(–Y) zone. Drawings of coronal sections (caudal to rostral) from cases mb6 (left), mb11 (middle), and mb18 (right) are shown. For additional details, see legend to Figure 5. See text for a detailed description. See list for abbreviations. Scale bar = 1 mm.

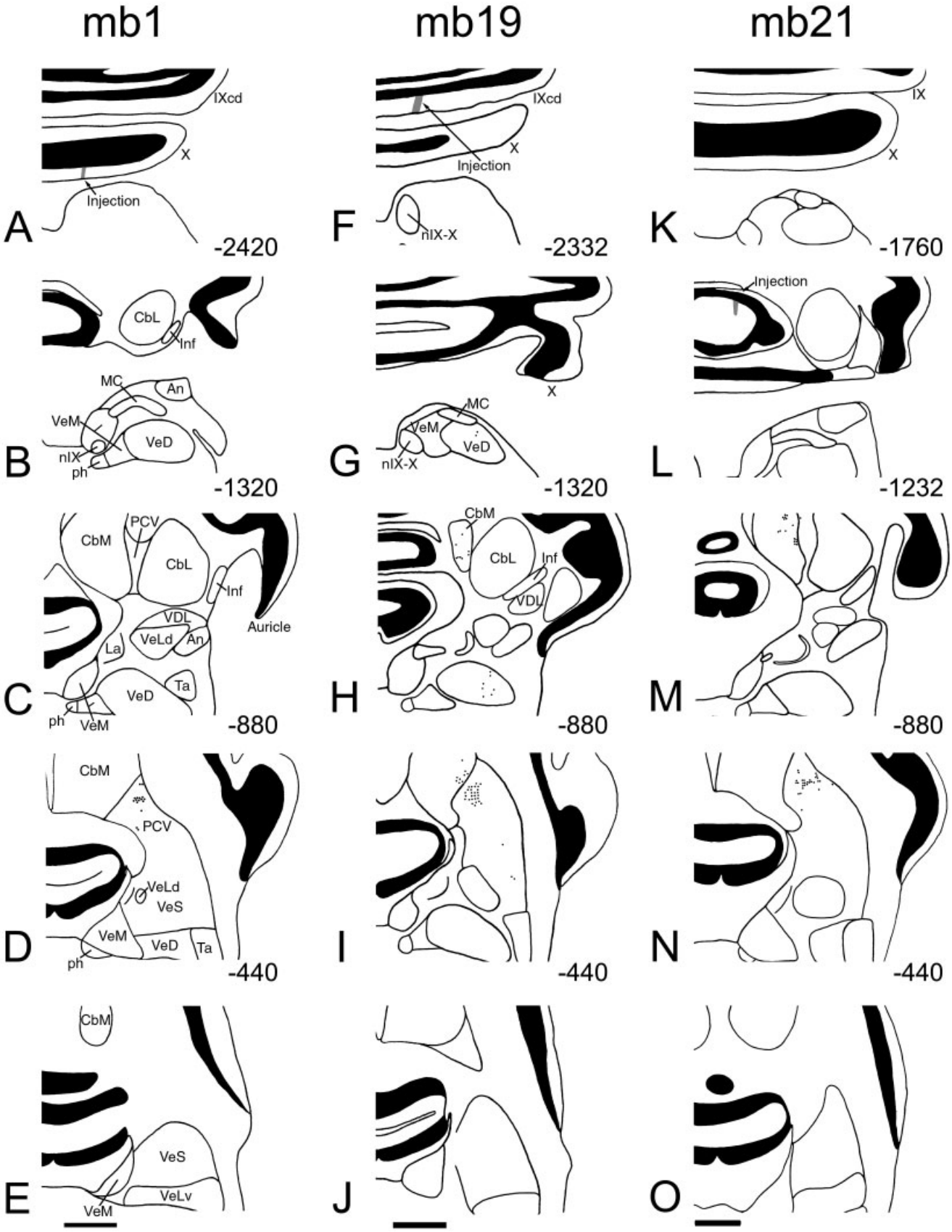

Fig. 8. **A–O:** Projections of Purkinje cells in the t(–X–Z) zone. Drawings of coronal sections (caudal to rostral) from cases mb1 (left), mb19 (middle), and mb21 (right) are shown. For additional details, see legend to Figure 5. See text for a detailed description. See list for abbreviations. Scale bars = 1 mm.

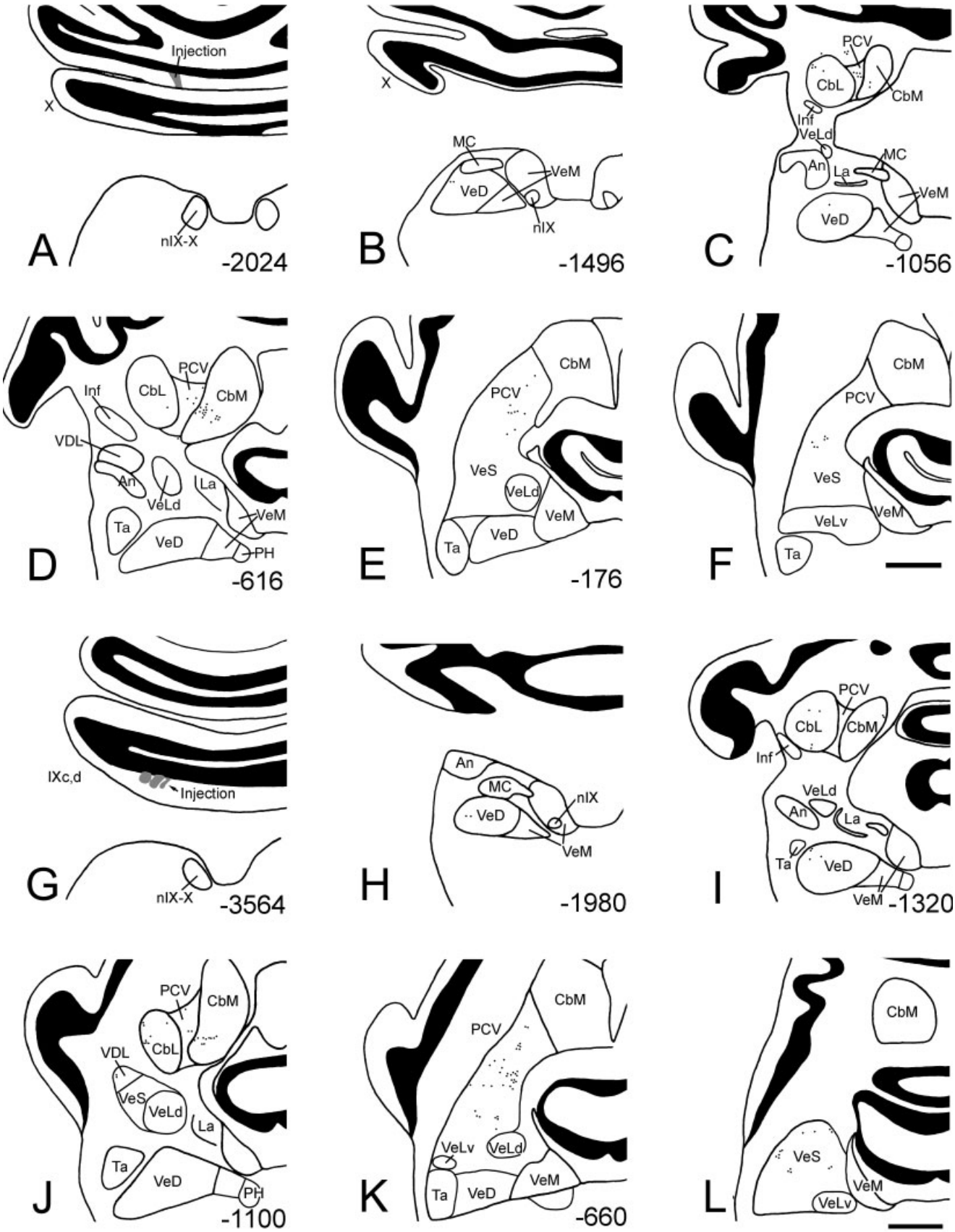

Fig. 9. **A–L:** Projections of Purkinje cells in the t(+Y) zone. Drawings of coronal sections (caudal to rostral) from cases MB22 (top; A–F) and BDA28 (bottom; G–L) are shown. For additional details, see legend to Figure 5. See text for a detailed description. See list for abbreviations. Scale bars = 1 mm.

zones containing rVA and rH45c cells (Kano et al., 1990), and Barmack and Shojaku (1995) reported that CSA was modulated in response to vestibular stimulation originating in the otolith organs. This contrasts with the CSA in the medial VbC of pigeons, which responds to patterns of optic flow resulting from self-translation along a particular axis (Wylie et al., 1993, 1998; Wylie and Frost, 1999a; see also Winship and Wylie, 2001). Given that the CSA is responsive to translational optic flow along the vertical axis [t(–Y) and t(+Y) cells] or an axis oriented 45° to the midline [t(–X–Z) and t(–X+Z) cells], the translational optic flow system uses a frame of reference similar to that used by the rotational optic flow system (Wylie et al., 1998; Wylie and Frost, 1999b).

Zonal organization of the translation cells in the medial VbC of pigeons

Previous electrophysiological studies (Wylie and Frost, 1999a; Crowder et al., 2000) suggested a zonal organization of the four response types in the medial VbC; however, this was based (largely) on qualitative observations involving oblique penetrations, lateral to medial through the VbC (see, e.g., Fig. 8 of Wylie and Frost, 1999a; Fig. 11 of Wylie et al., 1993). In Figure 3, the zonal organization of the medial VbC is shown from data obtained in the present study and previous neuroanatomical studies (Lau et al., 1998; Wylie et al., 1999a; Crowder et al., 2000). In confirmation of previous studies, the most medial zone and the adjacent zone are each about 0.5 mm in width and contain t(–X–Z) and t(–X+Z) cells, respectively. A third zone is about 0.8–1.0 mm in width and contains both t(+Y) and t(–Y) cells. Previous studies had suggested, with caution, that the t(+Y) cells were found lateral to the t(–Y) cells. Data from the present study do not support this but suggest that they are within a single zone. Alternatively, we could state that we have failed to show a medial-lateral distinction between the locations of the two cell types. However, although the sample is small in this regard, it appears that, in folia X, t(–Y) neurons are located in dorsal lamella, whereas t(+Y) neurons span both the dorsal and the ventral lamellae. Wylie et al. (1993) also noted an absence of +t(–Y) cells in ventral X.

Zonal projection of the ventral uvula and nodulus in pigeons

In the present study, we injected anterograde tracers into physiologically identified zones of the ventral uvula and nodulus in pigeons. Consistent with our previous study (Wylie et al., 1999a) of the projection of the medial VbC as a whole, we observed moderate to heavy terminal labeling in pcv, CbM, VeS, and VeD (see also Arends et al., 1991). Some labeling was also found in VeM, but only sparse labeling was found in CbL and Inf. In our previous study, we also noted sparse terminal labeling in VDL, Ta, and VeLv after injections into the medial VbC, but this was not seen in the present study.

This study has revealed a clear difference in the projections of the different zones, which we have summarized in Figure 10. The t(–X–Z) zone projected to the dorsal pcv abutting the CbM, and some labeling was found in the CbM. The t(–X+Z) zone also projected to the pcv and CbM, but to areas ventral to the projection sites of the t(–X–Z) zone. In Figure 10, the projection sites in the pcv and CbM of these two zones appear as nonoverlapping, but this is not necessarily the case. Injection sites where t(–Y) CSA was recorded projected ventrally in the pcv, the dorsal VeS, and the dorsolateral VeD and laterally in the caudal margin of the VeM. The pattern of projection of the two injection sites where t(–Y) CSA was recorded was similar to that observed for both t(–Y) and t(–X+Z) injections. However, we do not believe that the data set from t(+Y) injections is sufficient to draw any firm conclusions, so this is not included in Figure 10.

Unfortunately, not much is known about the pcv, the major projection site of all the zones. In Nissl-stained sections, the pcv is not well defined by distinct borders but is a diffuse collection of cells that bridge CbL, CbM, and dorsal VeS (Arends and Zeigler, 1991a; Karten and Hodos, 1967). This being the case, the pcv is understandably neglected or perhaps mislabelled as the CbM, CbL, or VeS in some studies (see, e.g., Schwarz and Schwarz, 1986; Dickman and Fang, 1996). Arends and Zeigler (1991b) reported that the pcv projects to premotor structures (see below). Wylie and colleagues (Wylie and Linkenhoker, 1996; Wylie et al., 1997) reported that mossy fibers from nBOR innervating the VbC send collaterals to the vestibular and cerebellar nuclei. Most of the mossy fiber collaterals terminated in the pcv and ventral CbM.

Possibility of retrograde labeling of mossy and climbing fiber collaterals

Although BDA of molecular weight 10,000 is regarded as a unidirectional (anterograde) tracer in pigeons (Veenman et al., 1992; Wild, 1993), Chen and Aston Jones (1998) have noted that the possibility of retrograde transport of BDA must be considered. Indeed, we did observe retrogradely labelled granule cells in the injected folium (Fig. 4A,B), presumably resulting from transport along damaged parallel fibers at the injection site. We have interpreted the presence of varicosities as the terminal labeling of Purkinje cell axons owing to anterograde transport of BDA. However, it is possible that these varicosities are the terminals of mossy fiber or climbing fiber collaterals resulting from retrograde transport of BDA. This is particularly problematic if the larger injection sites encroached upon the granular layer. However, it is unlikely that there was significant labeling of mossy and climbing fiber collaterals for the following reasons. First, retrogradely labelled cells were not seen in the inferior olive. Second, we never observed any retrogradely labelled cell bodies in the vestibular or cerebellar nuclei, even in the cases involving the larger injections. Finally, if the varicosities were terminal labeling of mossy fiber collaterals, this would have been present bilaterally. In all of the cases involving unilateral injections, varicosities were never seen contralateral to the injection sites.

Comparison with the projections of the mammalian ventral uvula and nodulus

Because the physiology of the ventral uvula and nodulus is so different in mammals and birds (see above), the comparative aspects of the projection to the cerebellar and vestibular nuclei should be interpreted with caution. As in the pigeon, in mammals the ventral uvula and nodulus project to the VeM, VeD, VeS, and fastigial nucleus, which is equivalent to the pigeon CbM. In mammals there are also projections to the prepositus hypoglossi, group Y (Inf in pigeons; Arends and Zeigler, 1991a), and ventral dentate nucleus (Voogd, 1964; Angaut and Brodal, 1967; Haines, 1977; Balaban, 1984; Epema et al., 1985; Bernard,

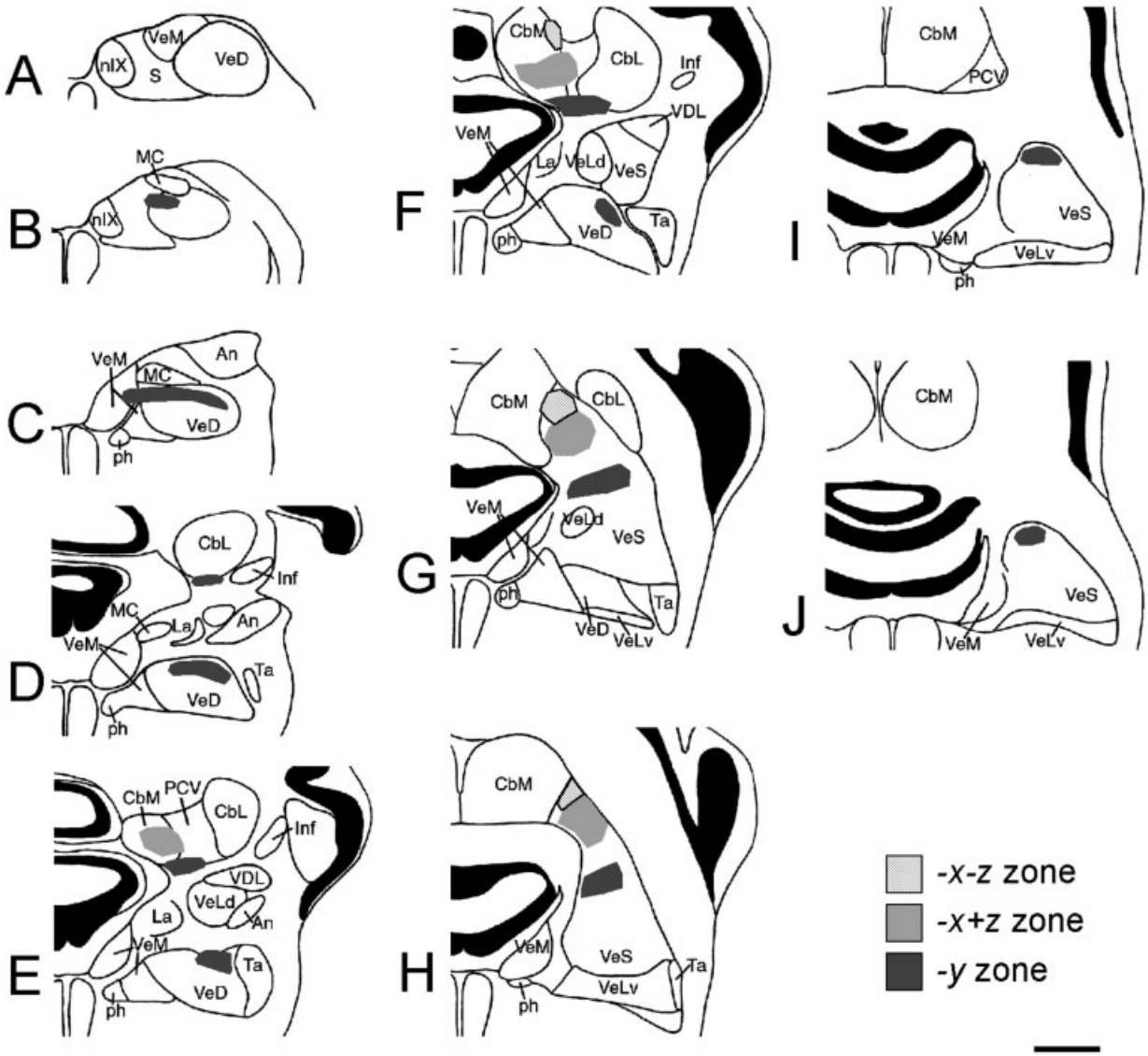

Fig. 10. Projections of t(–X–Z), t(–X+Z) and t(–Y) Purkinje cells in the medial vestibulocerebellum of pigeons. Drawings of coronal sections (caudal to rostral) through the vestibular and cerebellar nuclei are shown. The projections of the zones are represented by the stippled [t(–X–Z)], light gray [t(–X+Z)], and dark gray [t(–Y)] areas. This composite is based on the data from Figures 5–8. See text for a detailed description. See list for abbreviations. Scale bar = 1 mm.

1987; Shojaku et al., 1987; Wallberg and Dietrichs, 1988). In a study of the projections of the zones in the ventral nodulus in rabbits, Wylie et al. (1994) noted that there were numerous terminals outside the boundaries of the cerebellar nuclei in the peri-interpositus and peri-fastigial white matter. This could be equivalent to the projection to the pcv in pigeons (see also Haines, 1977).

Comparison with the projections of the pigeon flocculus

The pigeon flocculus is organized into four parasagittal zones, two rVA zones interdigitated with two rH45c zones (Winship and Wylie, 2003). The rVA zones project heavily to the central VeS, the VeM, and the prepositus hypoglossi (ph), whereas the rH45c zones project primarily to the Inf and the medial VeS (Wylie et al., 2003). It is possible that there are neurons in the vestibular nuclei that receive input from both flocculus and medial VbC Purkinje cells. In pigeons, the overlap of the projections of the t(–Y), rVA, and rH45c zones to the VeS appears minimal; each zone projects to distinct regions of the VeS: dorsal, central, and medial, respectively. The projections of the t(–Y) and rVA zones to the VeM appear not to overlap. The rVA zones project throughout the rostral two-thirds of the VeM, but the emphasis is ventral. The t(–Y) projection to the VeM is weak and is directed to the lateral margin in the caudal part of the nucleus. The projections of the t(–Y) and rVA zones to the VeD may overlap to a small degree. The rVA zones project throughout the VeD, although the emphasis is ventromedial, and there is little projection to the caudal VeD. The t(–Y) zones project to the dorsolateral VeD, where there is some input from the rVA zones.

Purkinje cells in the flocculus project primarily to preoculomotor structures (Wylie et al., 2003). Arends et al. (1991) found that the injections of WGA-HRP into the trochlear and oculomotor nuclei resulted in retrogradely labelled cells in all of the major projection sites of the flocculus, including Inf, medial VeS, VeM, and medial VeD. The findings of the present studies show that Purkinje cells in the medial VbC do not project extensively to preoculomotor structures. This is not surprising given the physiological distinction between the flocculus and the medial VbC and their roles in retinal image stabilization. CSA in the flocculus responds to optic flow induced by head rotation, which could be compensated for by rotational eye (and head) movements. CSA in the medial VbC responds to optic flow induced by self-translation, which would be compensated for by translatory head and/or body movements, such as the stereotypical head bobbing seen in pigeons (Freidman, 1975; Frost, 1978). Therefore, one would expect that the medial VbC projects to collimotor structures. The pcv projects to the red nucleus and throughout the vestibular nuclei, including the VeS, VeD, and VeM (Arends and Zeigler, 1991b), although it is not clear to which areas of these nuclei the pcv projects. As a whole, the CbM projects throughout the reticular formation, the red nucleus, the cervical areas of the spinal cord, and the vestibular nuclei. The projection of the CbM to the vestibular nuclei is especially strong to the caudal VeD. Vestibular nuclear projections to the neck motor column include the VeS and the VeD, primarily the caudal VeD (Wold, 1978; Arends and Zeigler, 1991b). Thus it appears that the medial VbC has extensive connections with premotor structures subserving the neck musculature.

Comparison with the primary projection from the vestibular apparatus

Given that the medial VbC responds to optic flow resulting from self-translation, one might expect that the projection sites of the medial VbC receive inputs from the otolith organs. Schwarz and Schwarz (1986) and Dickman and Fang (1996) provided detailed descriptions of the projections of the pigeon vestibular apparatus, which reveal that, to a certain extent, this expectation is met. The dorsal VeS receives a heavy input from the saccule and, to a lesser extent, the utricle. The VeD receives an extensive input from the utricle, with the emphasis directed laterally and caudally. The VeD also receives input from the saccule, especially caudally. The saccule and utricle both project to VeM, and this projection is restricted to the lateral half of VeM. Dickman and Fang (1996) report that the utricle projects to the lateral CbM and that the saccule projects to the ventrolateral CbM. Unfortunately, these two studies did not identify the pcv. From the drawings of Schwarz and Schwarz (1986), it is apparent that there is a light projection from the utricle to the pcv.

LITERATURE CITED

Angaut P, Brodal A. 1967. Anatomic study of vestibulocerebellar projections on vestibular nuclei in cats [in French]. J Physiol (Paris) 59(Suppl 4):327.

Arends JJA, Voogd J. 1989. Topographic aspects of the olivocerebellar system in the pigeon. Exp Brain Res Suppl 17:52–57.

Arends JJA, Zeigler HP. 1991a. Organization of the cerebellum in the pigeon (*Columba livia*): I. Corticonuclear and corticovestibular connections. J Comp Neurol 306:221–244.

Arends JJA, Zeigler HP. 1991b. Organization of the cerebellum in the pigeon (*Columba livia*): II. Projections of the cerebellar nuclei. J Comp Neurol 306:245–272.

Arends JJA, Allen RW, Zeigler HP. 1991. Organization of the cerebellum in the pigeon (*Columba livia*): III. Corticovestibular connections with eye and neck premotor areas. J Comp Neurol 306:273–289.

Balaban CD. 1984. Olivo-vestibular and cerebello-vestibular connections in albino rabbits. Neuroscience 12:129–149.

Barmack NH, Shojaku H. 1995. Vestibular and visual climbing fiber signals evoked in the uvula-nodulus of the rabbit cerebellum by natural stimulation. J Neurophysiol 74:2573–2589.

Bernard J-F. 1987. Topographical organization of olivocerebellar and corticonuclear connections in the rat—an WGA-HRP study: I. Lobules IX, X, and the flocculus. J Comp Neurol 263:241–258.

Blanks RH, Clarke RJ, Lui F, Giolli RA, Van Pham S, Torigoe Y. 1995. Projections of the lateral terminal accessory optic nucleus of the common marmoset (*Callithrix jacchus*). J Comp Neurol 354:511–532.

Brecha N, Karten HJ, Hunt SP. 1980. Projections of the nucleus of basal optic root in the pigeon: an autoradiographic and horseradish peroxidase study. J Comp Neurol 189:615–670.

Burns S, Wallman J. 1981. Relation of single unit properties to the oculomotor function of the nucleus of the basal optic root (AOS) in chickens. Exp Brain Res 42:171–180.

Chen S, Aston-Jones G. 1998. Axonal collateral-collateral transport of tract tracers in brain neurons: false anterograde labeling and useful tool. Neuroscience 82:1151–1163.

Clarke PGH. 1977. Some visual and other connections to the cerebellum of the pigeon. J Comp Neurol 174:535–552.

Collewijn H. 1975. Direction-selective units in the rabbit's nucleus of the optic tract. Brain Res 100:489–508.

Crowder NA, Winship IR, Wylie DRW. 2000. Topographic organization of inferior olive cells projecting to translational zones in the vestibulocerebellum of pigeons. J Comp Neurol 419:87–95.

Dickman JD, Fang Q. 1996. Differential central projections of vestibular afferents in pigeons. J Comp Neurol 367:110–131.

Epema AH, Guldemond JM, Voogd J. 1985. Reciprocal connections between the caudal vermis and the vestibular nuclei in the rabbit. Neurosci Lett 57:273–278.

Ezure K, Graf W. 1984. A quantitative analysis of the spatial organization of the vestibulo-ocular reflexes in lateral and frontal-eyed animals. I. Orientation of semicircular canals and extraocular muscles. Neuroscience 12:85–93.

Friedman MB. 1975. Visual control of head movements during avian locomotion. Nature 225:67–69.

Frost BJ. 1978. The optokinetic basis of head-bobbobg in the pigeon. J Exp Biol 74:187–195.

Gamlin PDR, Cohen DH. 1988. Projections of the retinorecipient pretectal nuclei in the pigeon (*Columba livia*). J Comp Neurol 269:18–46.

Giolli RA, Blanks RH, Torigoe Y. 1984. Pretectal and brain stem projections of the medial terminal nucleus of the accessory optic system of the rabbit and rat as studied by anterograde and retrograde neuronal tracing methods. J Comp Neurol 232:91–116.

Giolli RA, Blanks RHI, Torigoe Y, Williams DD. 1985. Projections of the medial terminal nucleus, ventral tegmental nuclei and substantia nigra of rabbit and rat as studied by retrograde axonal transport of horseradish peroxidase. J Comp Neurol 227:228–251.

Graf W, Simpson JI. 1981. The relations between the semicircular canals, the optic axis, and the extraocular muscle in lateral-eyed and frontal-eyed animals. In: Fuchs A, Becker W, editors. Progress in oculomotor research. Developments in neuroscience, vol 12. Amsterdam: Elsevier. p 409–417.

Graf W, Simpson JI, Leonard CS. 1988. Spatial organization of visual messages of the rabbit's cerebellar flocculus. II. Complex and simple spike responses of Purkinje cells. J Neurophysiol 60:2091–2121.

Grasse KL, Cynader MS. 1990. The accessory optic system in frontal-eyed animals. In: Leventhal A, editor. Vision and visual dysfunction, vol 4, the neuronal basis of visual function. New York: MacMillan. p 111–139.

Haines DE. 1977. Cerebellar corticonuclear and corticovestibular fibers of the flocculonodular lobe in a prosimian primate (*Galago senegalensis*). J Comp Neurol 174:607–630.

Holstege G, Collewijn H. 1982. The efferent connections of the nucleus of the optic tract and the superior colliculus in rabbit. J Comp Neurol 209:139–175.

Kano M, Kano M-S, Kusonoki M, Maekawa K. 1990. Nature of optokinetic

response and zonal organization of climbing fibre afferents in the vestibulocerebellum of the pigmented rabbit. II. The nodulus. Exp Brain Res 80:238–251.

Karten HJ, Hodos W. 1967. A stereotaxic atlas of the brain of the pigeon (*Columba livia*). Baltimore: Johns Hopkins Press.

Labendeira-Garcia JL, Guerra-Seijas MJ, Labendeira-Garcia JA, Jorge-Barreiro FJ. 1989. Afferent connections of the oculomotor nucleus in the chick. J Comp Neurol 259:140–149.

Larsell O. 1948. The development and subdivisions of the cerebellum of birds. J Comp Neurol 89:123–190.

Larsell O, Whitlock DG. 1952. Further observations on the cerebellum of birds. J Comp Neurol 97:545–566.

Lau KL, Glover RG, Linkenhoker B, Wylie DRW. 1998. Topographical organization of inferior olive cells projecting to translation and rotation zones in the vestibulocerebellum of pigeons. Neuroscience 85:605–614.

Leonard CS, Simpson JI, Graf W. 1988. Spatial organization of visual messages of the rabbit's cerebellar flocculus. I. Typology of inferior olive neurons of the dorsal cap of Kooy. J Neurophysiol 60:2073–2090.

Maekawa K, Takeda T. 1977. Afferent pathways from the visual system to the cerebellar flocculus of the rabbit. In: Baker R, Berthoz A, editors. Control of gaze by brain stem neurons, developments in neuroscience, vol. 1. Amsterdam: Elsevier. p 187–195.

Maekawa K, Takeda T. 1979. Origin of descending afferents to the rostral part of the dorsal cap of the inferior olive which transfers contralateral optic activities to the flocculus. A horseradish peroxidase study. Brain Res 172:393–405.

McKenna O, Wallman W. 1985. Accessory optic system and pretectum of birds: comparisons with those of other vertebrates. Brain Behav Evol 26:91–116.

Mizuno N, Mochizuki K, Akimoto C, Matsushima R. 1973. Pretectal projections to the inferior olive in the rabbit. Exp Neurol 39:498–506.

Ruigrok TJH, Osse RJ, Voogd J. 1992. Organization of inferior olivary projections to the flocculus and ventral paraflocculus of the rat cerebellum. J Comp Neurol 316:129–150.

Schwarz DWF, Schwarz IE. 1986. Projection of afferents from individual vestibular sense organs to the vestibular nuclei in the pigeon. J Comp Neurol 102:438–444.

Shojaku H, Sato Y, Ikarashi K, Kawasaki T. 1987. Topographical distribution of Purkinje cells in the uvula and the nodulus projecting to the vestibular nuclei in cats. Brain Res 416:100–112.

Simpson JI. 1984. The accessory optic system. Annu Rev Neurosci 7:13–41.

Simpson JI, Graf W. 1981. Eye-muscle geometry and compensatory eye movements in lateral-eyed and frontal-eyed animals. Ann N Y Acad Sci 374:20–30.

Simpson JI, Graf W. 1985. The selection of reference frames by nature and its investigators. In: Berhoz A, Melvill-Jones G, editors. Adaptive mechanisms in gaze control: facts and theories. Amsterdam: Elsevier. p 3–16.

Simpson JI, Soodak RE, Hess R. 1979. The accessory optic system and its relation to the vestibulocerebellum. Prog Brain Res 50:715–24.

Simpson JI, Graf W, Leonard CS. 1981. The coordinate system of visual climbing fibres to the flocculus. In: Fuchs AF, Becker W, editors. Progress in oculomotor research. Amsterdam: Elsevier. p 475–484.

Simpson JI, Giolli RA, Blanks RHI. 1988a. The pretectal nuclear complex and the accessory optic system. In: Buttner-Ennerver JA, editor. Neuroanatomy of the oculomotor system. Amsterdam: Elsevier. p 335–364.

Simpson JI, Leonard CS, Soodak RE. 1988b. The accessory optic system of rabbit. II. Spatial organization of direction selectivity. J Neurophysiol 60:2055–2072.

Simpson JI, Leonard CS, Soodak RE. 1988c. The accessory optic system: analyzer of self-motion. Ann N Y Acad Sci 545:170–179.

Simpson JI, Graf W, Leonard CS. 1989a. Three-dimensional representation of retinal image movement by climbing fiber activity. In: Strata P, editor. The olivocerebellar system in motor control. Experimental brain research supplement, vol 17. Heidelberg: Springer-Verlag. p 323–327.

Simpson JI, Van der Steen J, Tan J, Graf W, Leonard CS. 1989b. Representations of ocular rotations in the cerebellar flocculus of the rabbit. In: Allum JHJ, Hulliger M, editors. Progress in brain research, vol 80. Amsterdam: Elsevier. p 213–223.

Takeda T, Maekawa K. 1976. The origin of the pretecto-olivary tract. A study using horseradish peroxidase. Brain Res 117:319–325.

Tan J, Gerrits NM, Nanhoe RS, Simpson JI, Voogd J. 1995. Zonal organization of the climbing fibre projection to the flocculus and nodulus of the rabbit. A combined axonal tracing and acetylcholinesterase histochemical study. J Comp Neurol 356:23–50.

van der Steen J, Simpson JI, Tan J. 1994. Functional and anatomic organization of three-dimensional eye movements in rabbit cerebellar flocculus. J Neurophysiol 72:31–46.

Veenman CL, Reiner A, Honig MG. 1992. Biotinylated dextran amine as an anterograde tracer for single- and double-labeling studies. J Neurosci Methods 41:239–254.

Voogd J. 1964. The cerebellum of the cat. Assen: Van Gorcum.

Wallberg F, Dietrichs E. 1988. The interconnection between the vestibular nuclei and the nodulus: a study of reciprocity. Brain Res 449:47–53.

Weber JT. 1985. Pretectal complex and accessory optic system of primates. Brain Behav Evol 26:117–140.

Whitlock DG. 1952. A neurohistological and neurophysiological study of afferent fibre tracts and receptive areas of the avian cerebellum. J Comp Neurol 97:567–635.

Wild JM. 1993. Descending projections of the songbird nucleus robustus archistrialis. J Comp Neurol 338:225–241.

Winship IR, Wylie DRW. 2001. Responses of neurons in the medial column of the inferior olive in pigeons to translational and rotational optic flowfields. Exp Brain Res 141:63–78.

Winship IR, Wylie DRW. 2003. Zonal organization of the vestibulocerebellum in pigeons (*Columba livia*): I. Climbing fibre input to the flocculus. J Comp Neurol 456:127–139.

Winterson BJ, Brauth SE. 1985. Direction-selective single units in the nucleus lentiformis mesencephali of the pigeon (*Columba livia*). Exp Brain Res 60:215–226.

Wold JE. 1976. The vestibular nuclei in the domestic hen (*Gallus domesticus*). I. Normal anatomy. Anat Embryol 149:29–46.

Wold JE. 1978. The vestibular nuclei in the domestic hen (*Gallus domesticus*). IV. The projection to the spinal cord. Brain Behav Evol 15:41–62.

Wylie DRW. 2001. Projections from the nucleus of the basal optic root and nucleus lentiformis mesencephali to the inferior olive in pigeons (*Columba livia*). J Comp Neurol 429:502–513.

Wylie DR, Frost BJ. 1991. Purkinje cells in the vestibulocerebellum of the pigeon respond best to either translational or rotational wholefield visual motion. Exp Brain Res 86:229–232.

Wylie DR, Frost BJ. 1993. Responses of pigeon vestibulocerebellar neurons to optokinetic stimulation: II. The 3-dimensional reference frame of rotation neurons in the flocculus. J Neurophysiol 70:2647–2659.

Wylie DRW, Frost BJ. 1996. The pigeon optokinetic system: Visual input in extraocular muscle coordinates. Vis Neurosci 13:945–953.

Wylie DRW, Frost BJ. 1999a. Complex spike activity of Purkinje cells in the ventral uvula and nodulus of pigeons in response to translational optic flowfields. J Neurophysiol 81:256–266.

Wylie DRW, Frost BJ. 1999b. Responses of neurons in the nucleus of the basal optic root to translational and rotational flowfields. J Neurophysiol 81:267–276.

Wylie DRW, Linkenhoker B. 1996. Mossy fibres from the nucleus of the basal optic root project to the vestibular and cerebellar nuclei in pigeons. Neurosci Lett 219:83–86.

Wylie DR, Kripalani T-K, Frost BJ. 1993. Responses of pigeon vestibulocerebellar neurons to optokinetic stimulation: I. Functional organization of neurons discriminating between translational and rotational visual flow. J Neurophysiol 70:2632–2646.

Wylie DR, DeZeeuw CI, DiGiorgi PL, Simpson JI. 1994. Projections of individual Purkinje cells of physiologically identified zones in the ventral nodulus to the vestibular and cerebellar nuclei in the rabbit. J Comp Neurol 349:448–463.

Wylie DRW, Linkenhoker B, Lau KL. 1997. Projections of the nucleus of the basal optic root in pigeons (*Columba livia*) revealed with biotinylated dextran amine. J Comp Neurol 384:517–536.

Wylie DRW, Bischof WF, Frost BJ. 1998. Common reference frame for neural coding of translational and rotational optic flow. Nature 392: 278–282.

Wylie DRW, Lau KL Jr, Lu X, Glover RG, Valsangkar-Smyth M. 1999a. Projections of Purkinje cells in the translation and rotation zones of the vestibulocerebellum in pigeon (*Columba livia*). J Comp Neurol 413: 480–493.

Wylie DRW, Winship IR, Glover RG. 1999b. Projections from the medial column of the inferior olive to different classes of rotation-sensitive Purkinje cells in the flocculus of pigeons. Neurosci Lett 268:97–100.

Wylie DRW, Brown MR, Barclay RR, Winship IR, Crowder NA, Todd KG. 2003. Zonal organization of the vestibulocerebellum in pigeons (*Columba livia*): II. Projections of the rotation zones of the flocculus. J Comp Neurol 456:140–153.